

Experimental and Numerical Investigation of Temperature Distribution in Room with Displacement Ventilation

PETER STANKOV, *Professor, Department of Hydroaerodynamics and Hydraulic Machines, Technical University of Sofia, Bulgaria*

JORDAN DENEV, *Assistant Professor, Department of Hydroaerodynamics and Hydraulic Machines, Technical University of Sofia, Bulgaria*

MARTIN BARTAK, *Assistant Professor, Department of Environmental Engineering, Czech Technical University in Prague, Czech Republic*

FRANTISEK DRKAL, *Professor, Department of Environmental Engineering, Czech Technical University in Prague, Czech Republic*

MILOS LAIN, *Assistant Professor, Department of Environmental Engineering, Czech Technical University in Prague, Czech Republic*

JAN SCHWARZER, *Assistant Professor, Department of Environmental Engineering, Czech Technical University in Prague, Czech Republic*

VLADIMIR ZMRHA L, *PhD Student, Department of Environmental Engineering, Czech Technical University in Prague, Czech Republic*

ABSTRACT

The paper deals with the assessment of results from an improved form of the standard $k-\varepsilon$ model for buoyant room flows. This improved $k-\varepsilon$ model is based on the generalized gradient diffusion hypothesis of Daly and Harlow (1970). Results from the computations for three-dimensional flow are compared with temperature measurements performed by the authors in a laboratory room with displacement ventilation. The numerical results show a good agreement with the laboratory experiments, superior to the results from the standard $k-\varepsilon$ model. The improved $k-\varepsilon$ model showed also a better convergence behaviour than the standard $k-\varepsilon$ equation model. It is quite easy to implement it in every code.

I. INTRODUCTION

Buoyant flows in ventilated rooms set a good challenge to turbulence modelling. A great variety of turbulence models exist in the world of computational fluid dynamics (CFD) with different levels of complexity and accuracy. This paper deals with the extension of standard $k-\varepsilon$ model, which is based on the ideas from more advanced algebraic flux models. The proposed improvement of $k-\varepsilon$ model uses the generalized gradient diffusion hypothesis (GGDH) of Daly and Harlow (1970) but unlike Ince and Launder (1989) it is still based on the wall-functions approach. As it is shown in this paper, the improved $k-\varepsilon$ model is quite simple, numerically stable and it gives accurate results when compared to temperature measurements in a laboratory room with displacement ventilation.

Firstly, the paper gives a short theoretical description of both the standard k - ε turbulence model and the improved model based on the generalized gradient diffusion hypothesis (GGDH). Secondly, the laboratory room with displacement ventilation is presented and the experimental methods used by the authors are described. Then the results of temperature measurements are compared with those of numerical predictions using both the standard and the improved k - ε models. Conclusions about the accuracy and the convergence behaviour of the two modelling approaches give useful information for all those who are not satisfied with the use of standard k - ε model for buoyant room flows.

2. THEORETICAL BACKGROUND

2.1 Standard k - ε model of turbulence for isothermal flows

The standard k - ε model of turbulence is developed for isothermal flows and consists of the following two partial differential equations (summation over repeating indexes is assumed):

- equation for the turbulent kinetic energy k

$$\frac{\partial}{\partial x_i} \left[\rho u_i k - \left(\mu + \frac{\mu_t}{\sigma_k} \right) \frac{\partial k}{\partial x_i} \right] = P - \rho \varepsilon \quad (1)$$

- equation for the dissipation rate of turbulent kinetic energy ε

$$\frac{\partial}{\partial x_i} \left[\rho u_i \varepsilon - \left(\mu + \frac{\mu_t}{\sigma_\varepsilon} \right) \frac{\partial \varepsilon}{\partial x_i} \right] = \frac{\varepsilon}{k} (c_1 P - c_2 \rho \varepsilon) \quad (2)$$

where the production term P of the turbulent kinetic energy is presented by

$$P = -\rho \overline{u'_i u'_j} \frac{\partial u_i}{\partial x_j} \quad (3)$$

After applying the Boussinesq's approximation and rearrangement, we obtain:

$$P = \mu_t \left(\frac{\partial u_i}{\partial x_j} + \frac{\partial u_j}{\partial x_i} \right) \frac{\partial u_i}{\partial x_j} \quad (4)$$

In the above equations u_i and u_j are the mean velocity components, u'_i and u'_j are the velocity fluctuations, μ is the dynamic viscosity, ρ is the fluid density, σ is the Prandtl number. The turbulent viscosity μ_t is defined as $\mu_t = c_\mu \rho k^2 / \varepsilon$.

The turbulence model constants are:

$$c_\mu = 0.09; \quad c_1 = 1.44; \quad c_2 = 1.92; \quad \sigma_k = 1.0; \quad \sigma_\varepsilon = 1.3$$

2.2 Simple Gradient Diffusion Hypothesis (SGDH)

When buoyant flows are considered, the production term P from eq. (3) is modified to include also the buoyancy effects and becomes:

$$P = -\rho \overline{u'_i u'_j} \frac{\partial u_i}{\partial x_j} - \beta \rho g_i \overline{u'_i \theta'}$$

(5)

where β is the volumetric expansion coefficient and θ' is the temperature fluctuation.

Within the widely used simple gradient diffusion hypothesis (SGDH) the turbulent heat flux in the last term of the equation (5) is modelled by:

$$\overline{\rho u'_i \theta'} = -\frac{\mu_t}{\sigma_\theta} \frac{\partial \theta}{\partial x_i} \quad (6)$$

where θ is the temperature and σ_θ is the turbulent Prandtl number, taken as a constant.

Thus the buoyant part of the turbulent production (with g_1, g_2 usually equal to zero, $g_3 = g$ and $x_3 \equiv z$) becomes:

$$P_b = \beta g \frac{\mu_t}{\sigma_\theta} \frac{\partial \theta}{\partial z} \quad (7)$$

The SGDH is quite simple, easy to implement and as shown by Nielsen (1998) in some cases it significantly influences the predicted results. However, this quite simple equation has the following drawback: in the vertical shear layers driven by buoyancy the buoyant generation would vanish, if the vertical temperature gradient becomes zero (Ince and Launder, 1989). This applies for example to the flows in cavities or rooms heated from below in which the temperature distribution is almost uniform.

A very important feature for the numerical prediction of buoyant flows is the numerical stability of turbulence model. However, as stated by Nielsen (1998), it is known that SGDH may produce numerical instability and therefore commercial codes give the possibility to exclude it from the computations.

2.3 Generalized Gradient Diffusion Hypothesis (GGDH)

According to this hypothesis introduced by Daly and Harlow (1970), the turbulent heat flux is calculated from:

$$\overline{\rho u'_i \theta'} = -c_\theta \rho \overline{u'_i u'_j} \frac{\partial \theta}{\partial x_j} \quad (8)$$

The coefficient c_θ is usually set equal to $\frac{3}{2} c_\mu / \sigma_\theta$ in order to stay closer to the eddy-viscosity formulation (Ince and Launder, 1989).

2.4 Comments on the improved k - ε model used in the present study

Generalized gradient diffusion hypothesis could be viewed as the first term of the more comprehensive algebraic flux model described by Hanjalic et al. (1994):

$$\overline{\rho u'_i \theta'} = -C \frac{k}{\varepsilon} \left(\overline{\rho u'_i u'_j} \frac{\partial \theta}{\partial x_j} + \xi \overline{\rho u'_j \theta'} \frac{\partial u_i}{\partial x_j} + \eta \beta g_i \rho \overline{\theta'^2} \right) \quad (9)$$

where C , ξ and η are the model constants.

This algebraic flux model, besides the contribution from mean velocity gradients, accounts also for the mutual interaction between the different components of turbulent heat flux and the contribution due to temperature variance. Despite the fact that GGDH is a somewhat 'truncated' version of the last equation, according to Hanjalic (1994) it improves substantially the prediction of natural convection in high cavities.

An example of a model based on GGDH is the model of Ince and Launder (1989). In this work the authors neglect the streamwise gradient as unimportant in their two-dimensional study; therefore Hanjalic and Vasic (1993) call this modification the 'partially generalized gradient diffusion hypothesis'. Unlike the work of Ince and Launder (1989), in the present three-dimensional study all terms of eq. (8) are retained. Thus, in the present work the expression for the buoyancy production term will be (considering g_1 and g_2 set to zero, $g_3 = g$, and for ideal gas conditions $\beta = 1/[\theta + 273.15]$):

$$P_b = -\frac{1}{\theta + 273.15} g c_\theta \rho \overline{u'_3 u'_j} \frac{\partial \theta}{\partial x_j} \quad (10)$$

and after substitution

$$P_b = \frac{1}{\theta + 273.15} g \cdot 0.15 \cdot \frac{k}{\varepsilon} \left[\mu_t \left(\frac{\partial u_j}{\partial x_3} + \frac{\partial u_3}{\partial x_j} \right) - \frac{2}{3} \delta_{3j} \rho k \right] \frac{\partial T}{\partial x_j} \quad (11)$$

where δ_{3j} is the Kronecker delta, equal to 1 if $j = 3$, otherwise equal to zero.

In the $\{x, y, z\}$ coordinates we obtain:

$$P_b = \frac{1}{\theta + 273.15} g \cdot 0.15 \cdot \frac{k}{\varepsilon} \left[\mu_t \left(\frac{\partial u}{\partial z} + \frac{\partial w}{\partial x} \right) \frac{\partial T}{\partial x} + \mu_t \left(\frac{\partial v}{\partial z} + \frac{\partial w}{\partial y} \right) \frac{\partial T}{\partial y} + \left(2\mu_t \frac{\partial w}{\partial z} - \frac{2}{3} \rho k \right) \frac{\partial T}{\partial z} \right] \quad (12)$$

where u, v, w are the mean velocity components.

The main reason why to use formula (12) for the present improved k - ε model is that unlike eq. (7) it gives the vertical flux driven by horizontal temperature gradient in the presence of shear stress. As it is shown further, this improved k - ε model shows also a superior numerical stability for the studied three-dimensional flow.

Most often the advanced algebraic flux models as well as the model of Ince and Launder (1989) include low-Re number extensions (Launder and Sharma, 1974; Lam and Bremhorst, 1981) aiming at the improved prediction of the flow physics in the near-wall region. The equations for such models include damping functions, which are active in the regions near the wall while in the internal regions the flow remains unchanged. However, such an approach requires an increased number of numerical points near the wall considerably (up to 20-30 points in the very proximity of each wall). This prevents the algebraic flux models from being used for three-dimensional engineering predictions.

Three-dimensional engineering flows still need to use a kind of wall-functions near the wall in order to overcome the problem with large number of grid points, see e.g. the work of

Chikamoto et al. (1992). Therefore, in order to bring the present model as close to the needs of practical engineers as possible, the standard log-law wall-functions approach of Launder and Spalding (1974) are retained.

3. NUMERICAL PROCEDURE

In the present investigation a new version of the computational fluid dynamics (CFD) part of the ESP-r (Energy Systems Performance - research) software is utilized. The ESP-r software is developed for the purposes of the buildings energy performance analysis and the computational fluid dynamics part is added to enlarge its possibilities for integrated simulation together with the detailed air flows in rooms (Beausoleil-Morrison et al., 2001).

The CFD part uses the finite volume numerical method for the discretization of the partial differential equations on structured staggered numerical grids. The model includes the equations for temperature, the equations for the three velocity components and for the pressure correction segregated by the SIMPLEC algorithm. The k- ϵ turbulence model is used together with the wall-functions approach for the boundary conditions on rigid walls. Radiation between walls is not taken into account in the present study.

4. DESCRIPTION OF LABORATORY EXPERIMENTS

4.1 Test Room

The measurements were performed in a test room 4.2 m long, 3.6 m wide and 3 m high with displacement type of ventilation. The supply air opening 0.3 m x 0.2 m was placed symmetrically on the west wall having the bottom edge on the floor level. A special lemniscate-shaped inlet nozzle was designed in order to obtain inlet velocity profiles as uniform as possible. The outlet position was on the west wall 2.05 m above the floor.

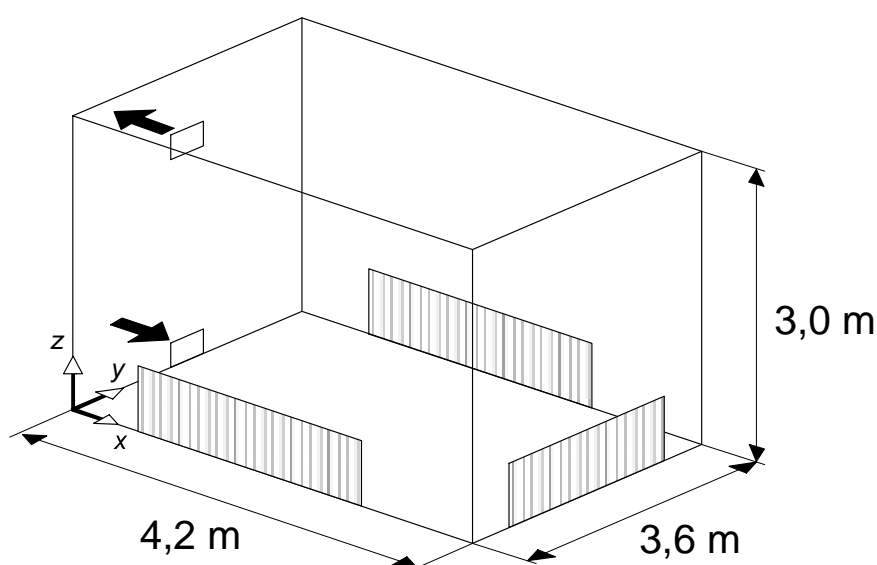


Figure 1: Schematic drawing of the test room (heat sources shown hatched)

The test room was insulated on the external surface in order to minimize the heat transfer through the room envelope. Three electric heating sheets were installed on the two longer walls and on the wall opposite to the air supply (see Fig. 1). Additional thermal insulation was applied between the room walls and heating sources.

4.2 Experimental conditions

The test room was placed in a bigger air-conditioned enclosure providing required external conditions for the experiments. Different locations of the surrounding enclosure were individually ventilated and heated by 4 heaters and 10 fans in order to obtain the room walls as adiabatic as possible according to the local air temperatures in the room (quasi-adiabatic walls). This occurred to be very difficult for the floor, which is partly cooled by supplied air.

The average inlet velocity (over the inlet section) was 0.84 m/s, yielding the ventilation rate of 4 ach. The temperature of supplied air was 20 °C with fluctuations ± 0.5 °C. The heating output of electric sheets was 240 W/m², which gives output 683 W in total for the three heaters.

4.3 Method and instrumentation

The temperature profiles were measured on 22 vertical lines, each of them having 22 measuring points. Up to four vertical multi-point probes with negative thermistors (NTC) were used at a time. The NTC probes were of 2.4 mm diameter and having a short time constant (10 s). Experimental data were collected in one-minute periods by the data acquisition unit Ahlborn ALMEMO 5590-3.

The radiation error in air temperature measurements was found negligible; there were no differences observed in measurements with and without reflective screens. The reason is in low surface temperatures of the heating panels (30 to 40 °C) compared to the air temperatures and in small-sized NTC sensors.

The temperatures were measured at 432 points in three vertical planes, out of them 168 points (8 vertical lines) in the middle longitudinal plane and the rest (14 vertical lines) on both sides of this plane.

4.4 Results and discussion

The results from simulation are available at any point of the 3D numerical grid while the measured data were obtained only in three vertical planes. The main part of measured points were placed in the middle longitudinal plane because the biggest differences between supplied air temperature and inner air temperature can be observed in this plane. Hence these results from this plane were used for the comparisons between the measured and numerically simulated data as they are given in the following Figures 2 to 4. The temperature profiles presented in Fig. 5 are selected from different vertical planes to show that the conclusions are valid not only for the middle plane.

Considering the temperature profiles shown in the Figure 5 both numerical methods show a very good agreement with the experimentally measured data. However, the generalized gradient diffusion hypothesis (GGDH) follows better the measurements in terms of overall temperature field pattern (see Figures 2 to 4). The simple gradient diffusion hypothesis (SGDH) produces temperature stratification, which is different from that in the laboratory experiment.

GGDH provides also slightly better convergence giving the residuals of the order of 10^{-4} (except for energy) after 6000 iterations while SGDH gave the residuals of the order of 10^{-3} .

Air temperatures: SGDH

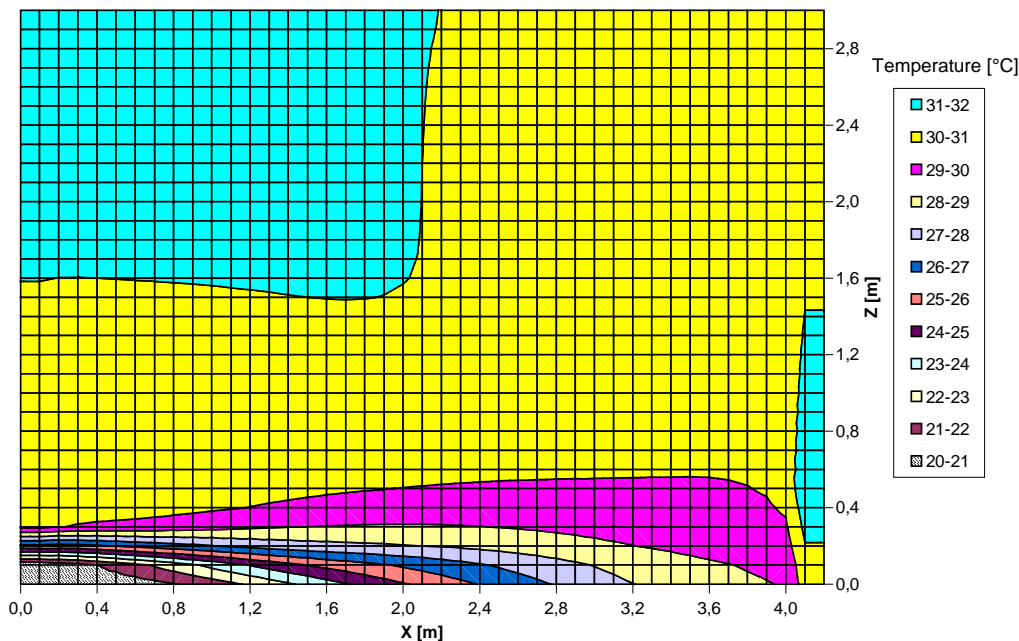


Figure 2: Air temperatures numerically simulated using the simple gradient diffusion hypothesis (SGDH); results in the middle longitudinal plane.

Air temperatures: GGDH

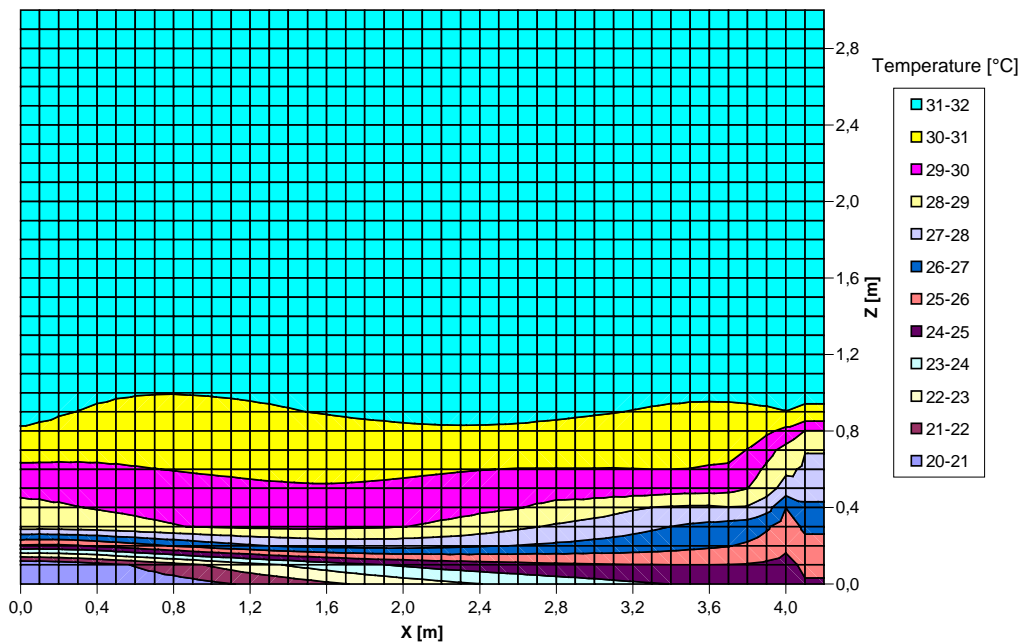


Figure 3: Air temperatures numerically simulated using the generalized gradient diffusion hypothesis (GGDH); results in the middle longitudinal plane.

Air temperatures: measured

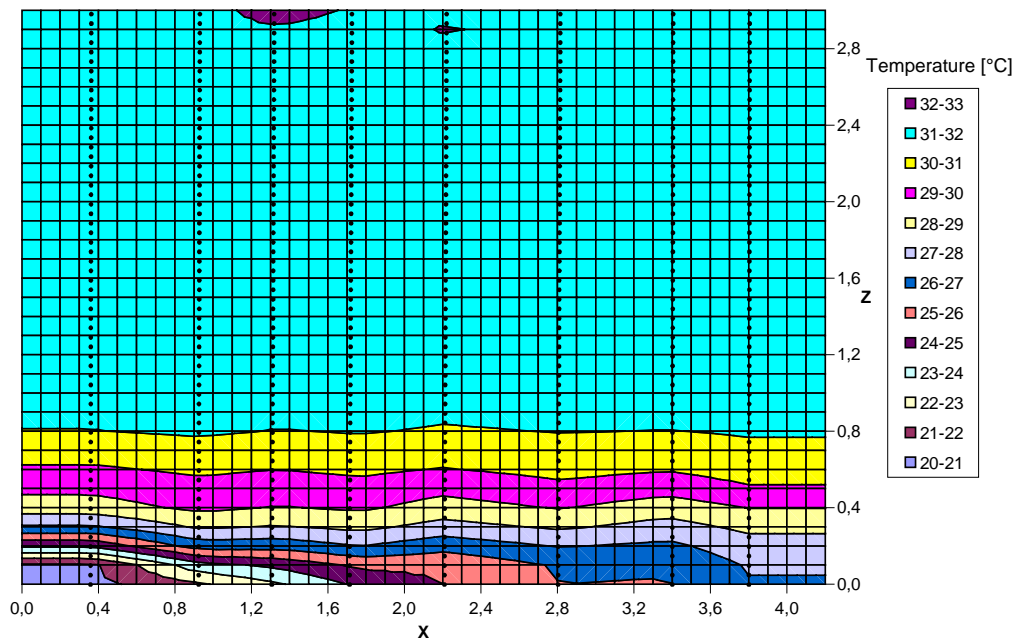


Figure 4: Air temperatures measured in the test room; results in the middle longitudinal plane.

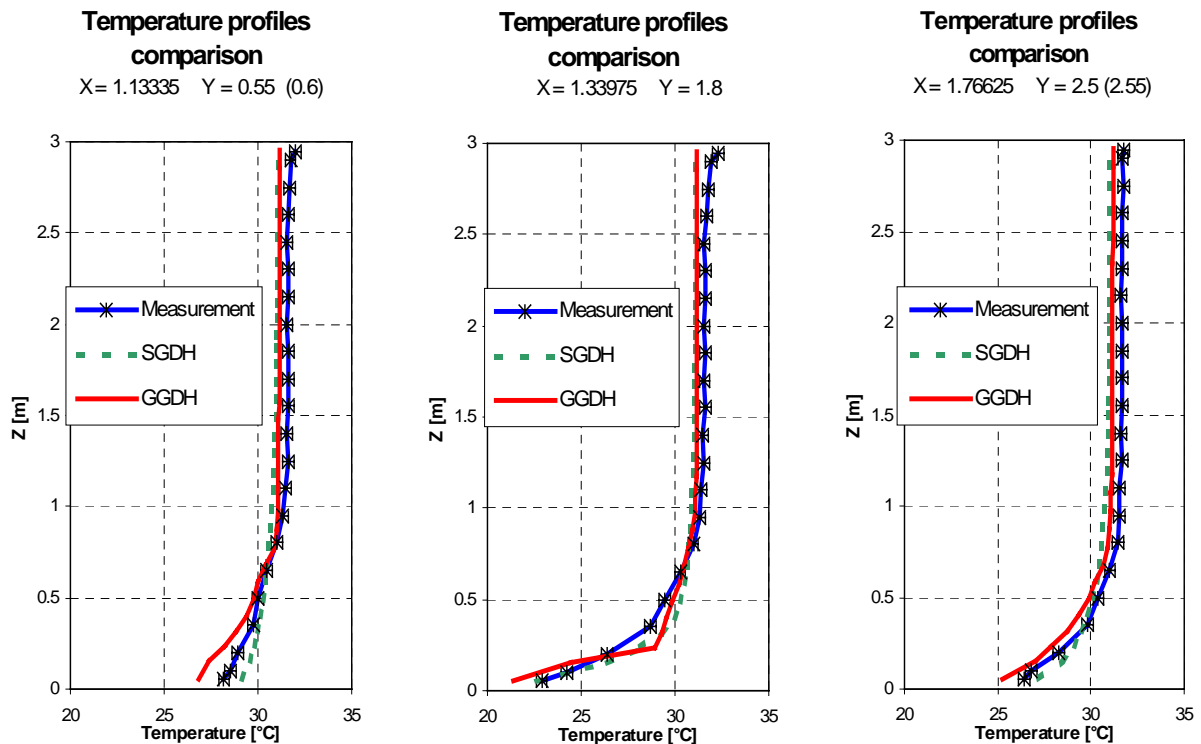


Figure 5: Air temperature profiles: comparison between the two numerical methods and the measured data (selected vertical lines)

5. CONCLUSIONS

An improved k-e model for buoyant flows is introduced and tested for ventilated rooms. The improved model, based on the GGDH is computationally more stable than the standard k-e model. It gives better results which are closer to the experiments for a three-dimensional room flow with displacement ventilation. It is very simple to upgrade the standard k-e model to the introduced improved form: all what is required from the user is the use of equation (12), instead of the equation (7).

Based on the more correct results and the most stable numerical behaviour the authors made the conclusion that this improved model will become standard for the new version of the CFD (Computational Fluid Dynamics) code used for buildings energy analysis as part of the ESP-r (Energy Systems Program-research) software.

6. ACKNOWLEDGEMENTS

This work was made with the financial support from the European Commission (INCO Copernicus project ERB IC15 CT989 0511) and the Czech Ministry of Education (project MSM 210000011).

REFERENCES

- Chikamoto, T., Murakami, S. and Kato, S. 1992. Numerical simulation of velocity and temperature fields within atrium based on modified k- ϵ model incorporating damping effect due to thermal stratification. *Proc. of International Symposium on Room Air Convection and Ventilation Effectiveness*. Tokyo, Japan.
- Beausoleil-Morrison, I., Clarke, J. A., Denev, J., Macdonald, I. A., Melikov, A., Stankov, P. 2001. Further developments in the conflation of CFD and building simulation. *Proc. of 7th International IBPSA Conference Building Simulation 2001*. Rio de Janeiro, Brasil.
- Daly, B. J. and Harlow, F. H. 1970. *Phys. Fluids*, vol. 13, 2634
- Hanjalic, K. and Vasic, S. 1993. Computation of turbulent natural convection in rectangular enclosures with an algebraic flux model. *Int. J. Heat Mass Transfer*, **36** (14), pp. 3603-3624.
- Hanjalic, K. 1994. Achievements and limitations in modelling and computation of buoyant turbulent flows and heat transfer. *Proceedings of the 10th International Heat Transfer Conference*, Vol. 1, pp. 1-18, Brighton, UK.
- Hanjalic, K., Kenjeres, S. and Durst, F. 1994. Numerical study of natural convection in partitioned 2-dimensional enclosures at transitional Rayleigh numbers. *Int. Symposium on Turbulence, Heat and Mass Transfer*, Lisbon, Portugal

Ince, N. Z. and Launder, B. E. 1989. On the computation of buoyancy-driven turbulent flows in rectangular enclosures. *Int. J. Heat and Fluid Flow*, **10** (2), pp. 110-117.

Lam, C.K.G. and K.A. Bremhorst 1981 'Modified form of the k-e model for predicting wall turbulence', *J. of Fluids Engng*, 103, 456-460

Launder, B. E. and Spalding, D. B. 1974. The numerical computation of turbulent flows. *Computer Methods in Applied Mechanics and Engineering*, **3**(2), pp. 269-289, reprinted in special issue (1990)

Launder, B.E. and B.I. Sharma 1974 'Application of the energy-dissipation model of turbulence to the calculation of flow near a spinning disc' *Letters in Heat and Mass Transfer*, 1, 131-138

Nielsen, P. 1998. Turbulence models for prediction of room airflow. in: *Room Air Movement Computation* - lecture course at the CFD Centre for Engineering Prediction and Design, pp. 75-93, Technical University of Sofia, Bulgaria.

Nurnberg, G., Wood, P. and Shoukri, M. 1994. Experimental and numerical turbulent buoyant flows in an enclosure. *Proceedings of the 10th International Heat Transfer Conference*, Vol. 7, pp. 119-124, Brighton, UK.